Magnetite-Silver Core-Shell Nanoparticles: Synthesis, Characterizes and Optical Properties

Majid Rashidi Huyeh (majid.rashidi@phys.usb.ac.ir)
University of Sistan and Baluchestan
Saeideh Balouchzahi
University of Sistan and Baluchestan
Mahdi Shafiee Afarani
University of Sistan and Baluchestan
Parisa Khajegi
University of Sistan and Baluchestan

Research Article

Keywords: Magneto-plasmonic, Core-shell nanoparticles, Nanofabrication, Effective medium theory

Posted Date: August 24th, 2022

DOI: https://doi.org/10.21203/rs.3.rs-1979107/v1

Magnetite-Silver Core-Shell Nanoparticles: Synthesis, Characterizes and Optical Properties

Majid Rashidi Huyeh[*a], Saeideh Balouchzahi[a], Mahdi Shafiee Afarani[b], Parisa Khajegi[a]

[a] Department of Physics, Faculty of Science, University of Sistan and Baluchestan, Zahedan, 9816745785, Iran.

[b] Department of Materials Engineering, Faculty of Engineering, University of Sistan and Baluchestan, Zahedan, 9816745845, Iran.

[*]Corresponding author E-mail: majid.rashidi@phys.usb.ac.ir

Abstract: Fe_3O_4 and Fe_3O_4/Ag core-shell nanocomposite powders were synthesized via the co-precipitation method. Structure, microstructure, magnetic, and optical properties of Fe_3O_4/Ag and Fe_3O_4 were studied. XRD patterns and Uv-Vis spectra showed that nanostructure Fe_3O_4 and Fe_3O_4/Ag particles were successfully synthesized. AFM and MFM mode micrographs of Fe_3O_4 and Fe_3O_4/Ag powders confirm the formation of Fe_3O_4 particles in the nano-scale range. Both Fe_3O_4 and Fe_3O_4/Ag composite powders represented the superparamagnetic behavior due to the formation of nano-sized Fe_3O_4 particles. Furthermore, in-situ synthesis of Ag on the surface of magnetite nanoparticles increased the particle size, resulting in a decrease in the saturation magnetization. Moreover, based on the Maxwell-Garnet effective medium theory, a theoretical model was developed to determine the optical properties of suspended core-shell nanoparticles. A very good agreement may be found between the theoretical and experimental results. In addition, the local electric field in the particles, evaluated using the numerical Finite Element Method, showed that the electric field in the magnetite core may be amplified up to 20 times at the symmetrical SPR wavelength mode, depending on the silver shell thickness.

Keywords: Magneto-plasmonic, Core-shell nanoparticles, Nanofabrication, Effective medium theory

1. Introduction

Noble metal nanostructures have attracted much attention thanks to their optical properties linked to the Surface Plasmon Resonance (SPR) phenomenon [1]. This phenomenon is related to the coherent oscillation of the free electrons of the metal and results in an exaltation of the local electric field at a wavelength, known as SPR wavelength. The SPR wavelength depends on the different parameters, especially on the shape and size of nanoparticles [2]. So these materials were proposed for various applications such as photonic devices [3-5], catalysts [6, 7], and biomedicines [8]. On the other hand, many researchers have interested in magnetite

nanoparticles due to their special properties and environmental compatibility [9-14]. However, their optical applications are limited because of their intrinsic optical properties. Perhaps, suitable nanostructures including the noble metal and the magnetite, at the same time, have been proposed by many groups to increase the desired properties [15-17]. In particular, the core-shell nanoparticles, including the magnetite and the noble metal, were studied for their optical and magneto-optical properties [18-20]. Thus, Fe_3O_4/Ag nanoparticles are employed in various application fields including; catalysts [21-23], sensors [24], antibacterial applications [25], cancer detection [26], and magnetic application [27-29]. Fe_3O_4/Ag and Fe_3O_4 can be synthesized by several methods such as Solvothermal/hydrothermal [30-32], Co-precipitation [33, 34], sol-gel [35], a combination of electrochemical and reduction methods [36], and solution combustion method [37].

The aim of the present study was the synthesis of Fe_3O_4/Ag composite nanopowders. First, Fe_3O_4 particles were prepared. Then, Ag particles were in-situ-synthesized in the presence of magnetite nanopowders via precipitation method in the presence of $NaHB_4$ reducer agent. Structure, microstructure, magnetic and optical properties of Fe_3O_4/Ag and Fe_3O_4 were then studied. Moreover, a theoretical model based on the effective medium theory was proposed to determine the optical properties of embedded core-shell nanoparticles. This model predicts the symmetrical and antisymmetrical SPR modes linked to the shell silver very well. In addition, the numerical approach, based on the Finite Element Method (FEM) in the frequency domain, is applied to evaluate the local electrical field at the SPR wavelengths.

2. Experimental Section/Methods

Magnetite powders were synthesized by co-precipitation method using Iron(III) chloride hexahydrate ($FeCl_3.6H_2O$, Merck), Iron(II) chloride tetrahydrate ($FeCl_2.4H_2O$, Merck) and silver nitrate ($AgNO_3$, Merck) as starting materials. Sodium borohydride ($NaBH_4$, Merck) was also used as a reducing agent.

2.1. Synthesis of Fe3O4 nanoparticles

Magnetite powders were synthesized based on the work of E. Tahmasebi and Y. Yamini [38]. Synthesis of Fe_3O_4 particles was carried out in a 500 ml three-necked round glass flask under N_2 atmosphere together with reflux condition. First, 8.48 g Iron(III) chloride hexahydrate and 2.25g Iron(II) chloride tetrahydrate were dissolved in 400 ml of deionized water under magnetic stirring at 80°C. Then 20 ml of diluted ammonia (25 vol.%, Merck) was added drop-wise to the solution for 5 min until a black precipitate was obtained. The gained product was

washed with deionized water several times. Finally, the powders were dried in an electric oven at 70°C for 2 hours.

2.2. Synthesis of Fe3O4/Ag nanocomposite particles

First 1g of synthesized magnetite was added to 20 ml of $AgNO_3$ (0.885 molar) solution and agitated (1000 rpm) for 30 min. Then 50 ml of $NaBH_4$ (3.172 molar) was added drop-wise to the solution for 30 min until a dark olive green precipitate was obtained. Then, the synthesized powders were washed with deionized water several times and dried in an electric oven at 70°C for 2 hours.

In some cases, Ag particles were synthesized solely by removing nano magnetite particles from the reactor flask.

Structural characterization of the samples was performed using the X-ray diffraction (XRD, Bruker Advance D8) technique. The mean magnetite crystallite diameter ($d_{Scherrer}$) was determined from half-height width (β) of the (311) diffraction peak of magnetite using the Scherrer equation ($d_{Scherrer}=0.9\lambda/\beta \cos\theta$). One T80 UV–Vis spectrophotometer (PG Instruments Ltd) was applied to measure UV–visible absorption spectra. Scanning probe microscope with Atomic force and magnetic force modes (AFM/MFM, Ara research co. Iran) were used for topographic and fly phase of magnetic characterizations. The magnetic behavior of powders was characterized using the Vibration Sample Magnetometer (VSM, Meghnatis Daghigh Kavir Co., Kashan, Iran).

3. Results and Discussion

Figure 1 shows the XRD patterns of Fe_3O_4 and Fe_3O_4/Ag nanopowders. As illustrated, magnetite (card no. 01-076-1849) is the dominant phase for Fe_3O_4 powders. Moreover, Fe_3O_4/Ag contained magnetite and silver (card no. 01-087-0717) phases. Since Ag was synthesized on the surface of the Fe_3O_4 particles, the magnetite peak intensities decreased considerably. The broadening of magnetite peaks is due to the nanocrystalline nature of the magnetite powders with a mean crystallite size of 10.1 nm.

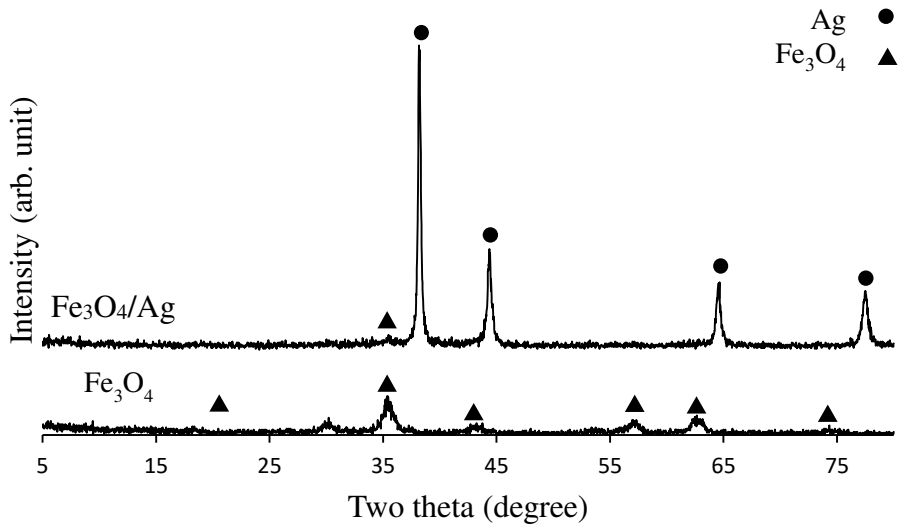

Figure 1. XRD patterns of Fe_3O_4 and Fe_3O_4/Ag nanopowders.

AFM and MFM mode micrographs of Fe_3O_4 and Fe_3O_4/Ag powders are shown in Figures 2a-d. The dark fleshes in Figures 2a and 2b indicate the magnetite nanoparticles. Considering of AFM mode micrograph of Fe_3O_4 powders (bright areas in Figure 2a) confirms the formation of Fe_3O_4 particles in the nano-scale range. Correspondingly, the magnetic nature of these particles can be observed in the MFM mode micrograph (dark areas in Figure. 2b). Moreover, in-situ synthesis of Ag on the surface of magnetite nanoparticles increased particle dimensions (Figure 2c) and so resulted in a decrease in magnetic behavior (Figure. 2d). These magnetic behaviors were studied by VSM mesurearements.

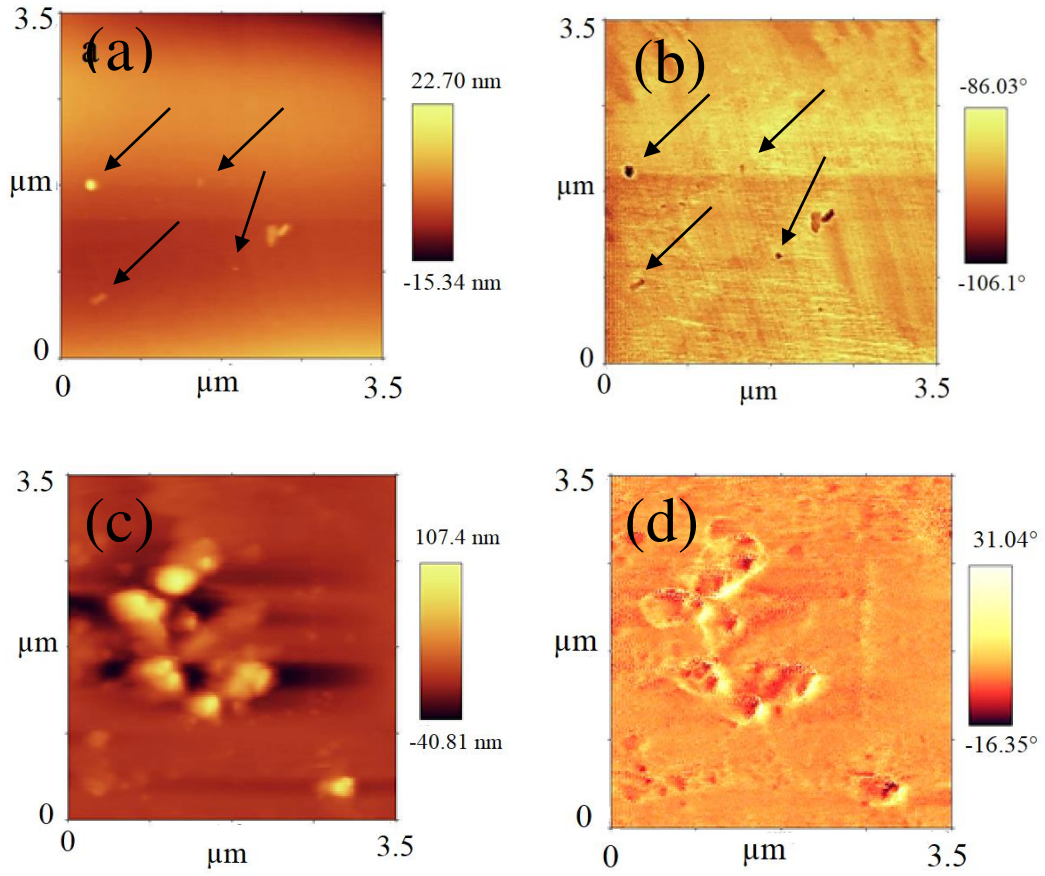

Figure 2. a) AFM mode micrograph of Fe_3O_4, b) MFM mode micrograph of Fe_3O_4, c) AFM mode micrograph of Fe_3O_4/Ag, and d) MFM mode micrograph of Fe_3O_4/Ag powders. The dark arrows in figures a and b indicate the magnetite nanoparticle on the surface.

Magnetization of Fe_3O_4 and Fe_3O_4/Ag powders as a function of the applied magnetic field at room temperature is shown in Figure 3. As illustrated, both samples show superparamagnetic behavior due to the formation of nano-sized Fe_3O_4 particles. Moreover, saturation magnetization values of the Fe_3O_4 and Fe_3O_4/Ag powders at 15 kOe field were about 30 and 20 emu.g^{-1}, respectively. These values are accorded to the results reported by Pastula et al. [39] As expected, the covering of Fe_3O_4 powders with Ag resulted in a decrease in saturation magnetization.

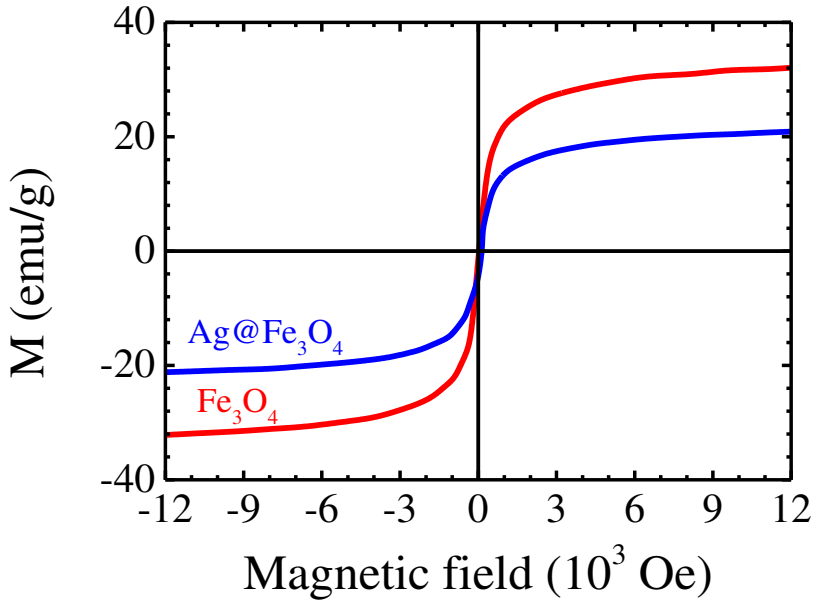

Figure 3. VSM diagram of Fe3O4 (red curve) and Fe3O4/Ag (blue curve) nanoparticles.

UV–visible absorption spectra of Ag, Fe_3O_4, and Fe_3O_4/Ag powders are shown in Figure 4. Fe_3O_4 absorbance decreases gradually with the wavelength that confirms the formation of Fe_3O_4 in nano-scale dimensions [40]. As illustrated, the Ag absorbance spectrum (red curve) presents a maximum value at 400 nm of wavelength. This peak is associated with the surface plasmon resonance effect of Ag nanoparticles [41]. Also, the Fe_3O_4/Ag spectrum (blue curve) presents two peaks at 435 and 780 nm of wavelengths, attributed to asymmetric and symmetric surface plasmon resonance, respectively [42,43].

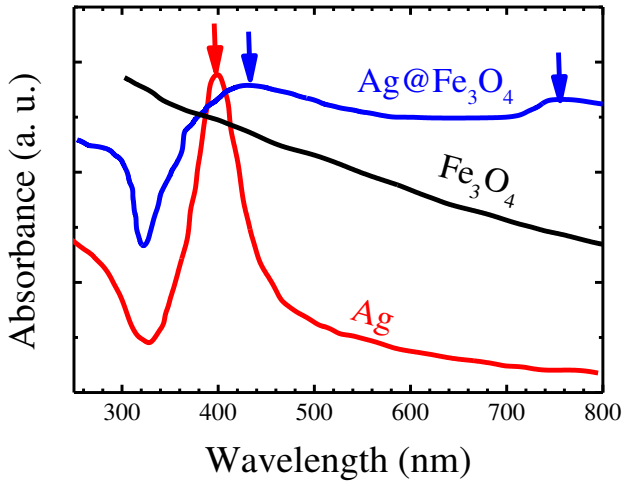

Figure 4. Absorbance spectra of suspended Fe3O4 (black), Ag (red), and Fe3O4/Ag (blue) nanoparticles. The red and blue arrows indicate the corresponding SPR wavelengths.

4. Model

The optical properties of suspended core-shell magnetite-silver nanoparticles were studied using the Maxwell-Garnet effective medium theory. This approximation is valid for a negligible scattering nanocomposite material, including the low volume fraction of nanoparticles embedded in a host medium as the following:

$$\tilde{\varepsilon}_{eff} = \varepsilon_d \frac{2(1-p)\varepsilon_d + (2p+1)\tilde{\varepsilon}_p}{(2+p)\varepsilon_d + (1-p)\tilde{\varepsilon}_p} \quad (1)$$

where, p, ε_d and $\tilde{\varepsilon}_p$ are nanoparticle volume fraction, dielectric function of host medium and the core-shell magnetite-silver nanoparticle, respectively. This earlier may be given using the effective medium theory for spheres multilayer [44]:

$$\tilde{\varepsilon}_p = \frac{A_2}{A_1}, \quad (2a)$$

$$\tilde{A}_1 = \left[(\tilde{\varepsilon}_c - \tilde{\varepsilon}_{sh})(1-\delta) + \tilde{\varepsilon}_{sh}\right] / \tilde{\varepsilon}_{sh} \quad (2b)$$

$$\tilde{A}_2 = \left[\tilde{A}_1 \tilde{\varepsilon}_{sh} + (\tilde{\varepsilon}_c - \tilde{\varepsilon}_{sh})\delta\right] / \tilde{\varepsilon}_{sh} \quad (2c)$$

where, $\tilde{\varepsilon}_c$ and $\tilde{\varepsilon}_{sh}$ are the dielectric function of magnetite core and that the silver shell, and $\delta = (R_c / R_{sh})^3$ represents the volume ratio of magnetite core to the particle volume. The absorbance then may be given as:

$$\alpha = \frac{4\pi}{\lambda} \mathrm{Im}\left(\sqrt{\tilde{\varepsilon}_{eff}}\right) \quad (3)$$

The model was applied to evaluate the optical properties of the core-shell magnetite-silver nanoparticle suspended in the water. The magnetite radius was considered 10 nm for the different silver shell thicknesses of 2, 5, and 10 nm. Based on the model, the absorbance spectra of different core-shell magnetite-silver nanoparticles were depicted in Figure 5. The absorbance of the magnetite and silver nanoparticles suspended in the water are also shown in Figure 5. The magnetite nanoparticle absorbance is magnified by a factor of 50. As illustrated, the absorbance of suspended magnetite NPs regularly decreases by wavelength, while for the suspended silver NPs, it shows a maximum value at about 400 nm of wavelength. This maximum is related to the Surface Plasmon Resonance phenomena [2]. As can be observed,

the absorbance of the core-shell magnetite-silver NPs presents two maxima. These maxima are linked to the combination of the dark and bright modes of SPR [39, 40, 45]. Indeed, the first pic of SPR, located at the shorter wavelength, is due to the antisymmetric combination of the dark and bright mods. In contrast, the second SPR pic, located at the longer wavelength, is related to the symmetrical combination of the dark and light mods. Comparing experimental works (Figure 4) and theoretical calculations (Figure 5) confirms the model assumptions and calculations. Figure 6 schematically represents the symmetrical and antisymmetric combination of dark and bright modes. The finite element method was also used for the study of the absorption cross-section as well as the electrical field in the nanoparticle according to reference 2. The local field in the particle for symmetrical and antisymmetric SPR mods for different shell thicknesses is depicted in Figure 7. The local field in the core for the symmetrical mode is much higher for each particle than that of the antisymmetric mode. This behavior can also explain the higher amplitude of the symmetrical mode compared to the antisymmetric mode. By increasing the shell thickness, the first maximum, located at the low wavelength, presents a slightly red-shift displacement, whereas the second one, located at the longer wavelength, reveals an important blue-shift. Indeed, for a very thin shell thickness, there is a high electric coupling between the dark and bright modes of SPR. By increasing the silver shell thickness, the distance between the inner and outer of the silver shell surfaces increases. Therefore, the electric coupling becomes weaker. As the magnetite core size is considered the same for different shell thicknesses, the first SPR mode is slightly affected by the shell thickness. In addition, the SPR amplitude increases by increasing the shell thickness.

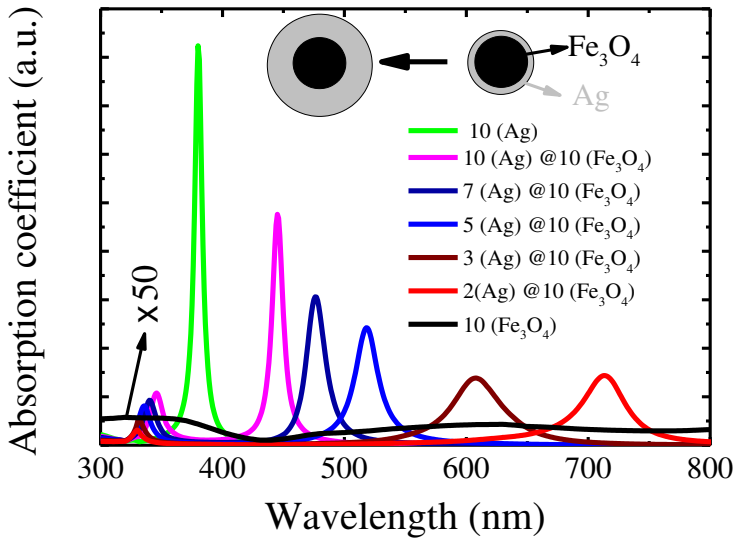

Figure 5- Absorption coefficient of magnetite-silver core-shell nanoparticle embedded in the water.

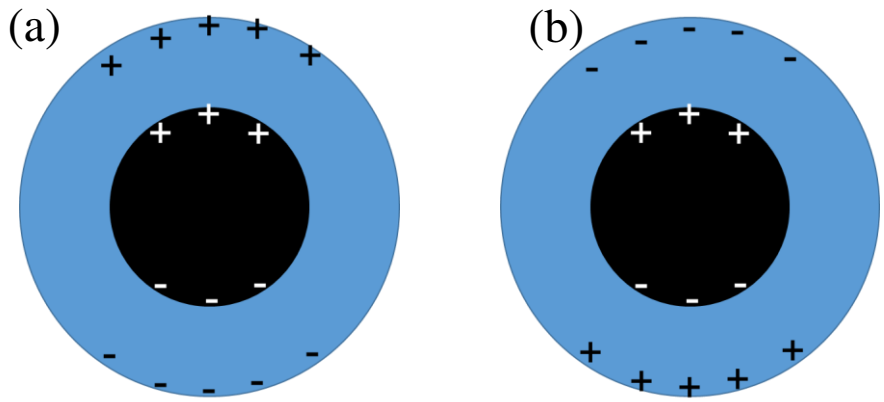

Figure 6- Scheme of symmetry (a) and antisymmetry (b) combination of dark and bright modes in the core-shell nanoparticle.

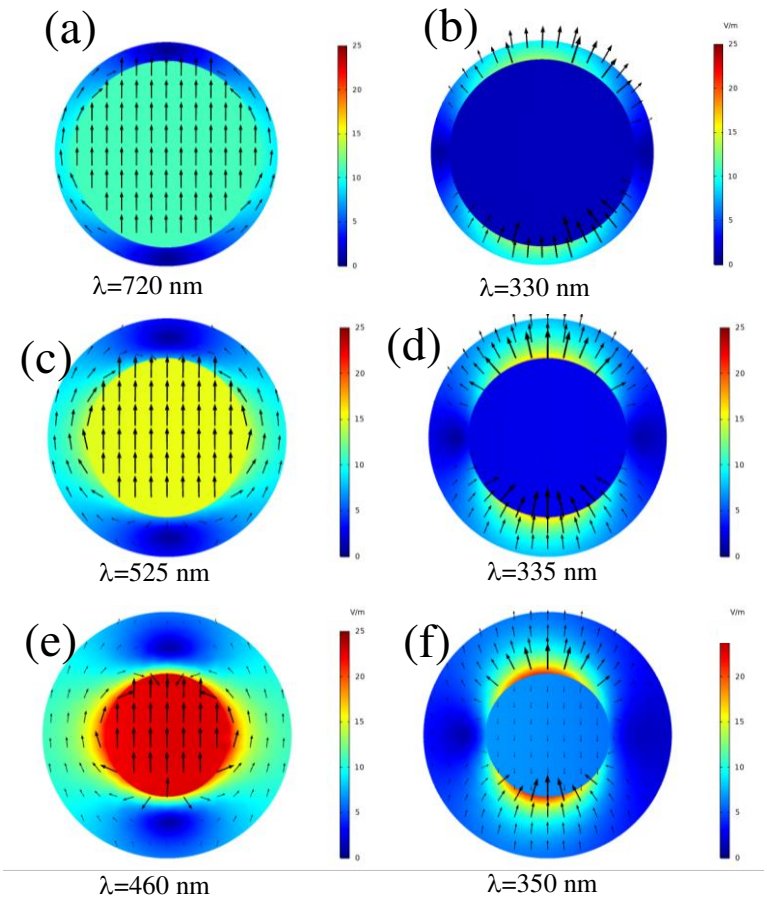

Figure 7- Local electric field distribution in the magnetite-silver core-shell nanoparticle at symmetry (a, c, and e) and antisymmetry (b, d, and f) SPR wavelengths for different shell thicknesses of 2 (a and b), 5 (c and d), and 10 (e and f) nm. Dark vectors represent the electric field.

5. Conclusion

The present work aimed to synthesize Fe_3O_4 and Fe_3O_4/Ag composite nanopowders via the co-precipitation method. Structure, microstructure, magnetic and optical properties of Fe_3O_4/Ag and Fe_3O_4 were studied. Moreover, a theoretical model was proposed to determine the optical properties of core-shell nanoparticles embedded in a host medium. Also, numerical FEM was used for the study of the electric local field in the particle. The main results can be concluded as follows

1- XRD patterns and Uv-Vis spectra showed that nanostructure Fe_3O_4 and Fe_3O_4/Ag particles could be successfully synthesized.

2- AFM and MFM mode micrographs of Fe_3O_4 and Fe_3O_4/Ag powders confirm the formation of Fe_3O_4 particles in the nano-scale range.

3- Both Fe_3O_4 and Fe_3O_4/Ag composite powders represented the superparamagnetic behavior due to the formation of nano-sized Fe_3O_4 particles. In-situ synthesis of Ag on the surface of magnetite nanoparticles increased particle sizes, resulting in a decrease in magnetic behavior.

4- Theoretical model predicts well two modes of symmetry and asymmetry SPRs. By increasing the silver shell thickness, symmetrical mode presents a blueshift and its amplitude increases.

5- Electric local field, calculated by FEM, showed amplification of the electric local field in the particle at the symmetric SPR wavelength mode depending on the silver shell thickness.

Acknowledgments

The authors would like to thank Mohammad Azari Nadjaf Abad from Karlsruhe Institute of Technology and Anh Van Le from the University of Tuebingen for their scientific comments.

Declarations

This work was supported by the University of Sistan and Baluchestan, Iran. The authors declare that no funds, grants, or other support were received during the preparation of this manuscript.

Conflict of interest

The authors have no potential conflicts of interest. The present research involved no human and/or animal participants. The authors have no relevant financial or non-financial interests to disclose.

Research Data Policy and Data Availability Statements

The datasets generated during and/or analyzed during the current study are available from the corresponding author on reasonable request.

Author Contributions

All authors contributed to the study conception and design. Material preparation, data collection and analysis were performed by Majid Rashidi Huyeh, Saeideh Balouchzahi, Mahdi Shafiee Afarani, and Parisa Khajegi. The first draft of the manuscript was written by Majid Rashidi Huyeh and Mahdi Shafiee Afarani, and all authors commented on previous versions of the manuscript. All authors read and approved the final manuscript.

References

[1] B. Palpant, in Gold Nanoparticles for Physics, Biology and Chemistry, edited by C. Louis and O. Pluchery (Imperial College Press, London, 2012), pp. 75–102, https://doi.org/10.1002/anie.201309807
[2] Parisa Khajegi and Majid Rashidi Huyeh (2021), https://doi.org/10.52547/ijop.15.1.41
[3] Wojciech Lesniak, Anna U. Bielinska, Kai Sun, Katarzyna W. Janczak, Xiangyang Shi, James R. Baker, and Lajos P. Balogh, Nano Lett. (2005), https://doi.org/10.1021/nl051077u
[4] C. H. Liu, Z. D. Zhou, X. Yu, B. Q. Lv, J. F. Mao, and D. Xiao, Anal Chem. (2005), https://doi.org/10.1134/S002016850803014X.
[5] Kunhao Li, Zhengtao Xu, Hanhui Xu, Patrick J. Carroll, and James C. Fettinger, Inorganic Chemistry (2006), https://doi.org/10.1021/ic051135e.
[6] T. Endo, T. Yomokazu, and K. Esumi, J. Colloid Interface Sci. (2005), https://doi.org/10.1016/j.jcis.2005.01.057.
[7] L. L. Tan, M. Wei, L. Shang, and Y.W. Yang, Adv. Funct. Mater. (2021), https://doi.org/10.1002/adfm.202007277
[8] Xuan Yang, Miaoxin Yang, Bo Pang, Madeline Vara, and Younan Xia, Chem. Rev. (2015), https://doi.org/10.1021/acs.chemrev.5b00193
[9] M. Arturo, Q. Lopez, and R. Jose, J. Colloid Interface Sci., (1993) https://doi.org/10.1006/jcis.1993.1277.
[10] C. L. Chiang, and C. S. Sung, J. Magn. Magn. Mater. (2006), https://doi.org/10.1016/j.jmmm.2005.08.022.
[11] K. Aoshima, and S. X.Wang, J. Appl. Phys. (2003), https://doi.org/10.1063/1.1558633
[12] S. A. Morton, G. D.Waddill, S. Kim, Ivan K Schuller, S.A Chambers, J.G Tobin, Surf. Sci., (2002), https://doi.org/10.1016/s0039-6028(02)01824-1.
[13] O. N. Shebanova, and P. Lazor, J. Chem. Phys. (2003), https://doi.org/10.1063/1.1602072.

[14] D. Schrupp, M. Sing, M. Tsunekawa, H. Fujiwara, S. Kasai, A. Sekiyama, S. Suga, T. Muro, V.A.M. Brabers, R. Claessen, Europhys. Lett. (2005), https://doi.org/10.1209/epl/i2005-10045-y.
[15] Z. B. Huang, and F. Q.Tang, , Preparation, Structure, and Magnetic Properties of Polystyrene Coated by Fe3O4 Nanoparticles, J. Colloid Interface Sci. (2004), https://doi.org/10.1016/j.jcis.2003.12.065.
[16] Y. L. Cui, D. D. Hu, Y.Fang, and J. B. Ma, Sci. China, Ser. B (2001), https://doi.org/10.1007/BF02879815.
[17] T. Shimizu, Y. Kitayama, and T. Kodama, Energy Fuels (2001), https://doi.org/10.1021/ef000200w.
[18] L. León Félix, J. A. Coaquira, M. A. Martínez, G. F. Goya, J. Mantilla, M. H. Sousa, L. L. Valladares, C. H. Barnes, and P. C. Morais, Scientific reports (2017), https://doi.org/10.1038/srep41732
[19] H. Salehizadeh, E.Hekmatian, M. Sadeghi, and K. Kennedy, J Nanobiotechnol (2012), https://doi.org/10.1186/1477-3155-10-3
[20] W. Brullot, V.K. Valev, T. Verbiest,. Nanomedicine: NBM (2012); https://doi.org/10.1016/j.nano.2011.09.004
[21] Guozhen Wang, Fei Li, Lan Li, Jiayu Zhao, Xinxuan Ruan, Wenping Ding, Jie Cai, Ang Lu, and Ying Pe, ACS Omega (2020), https://doi.org/10.1021/acsomega.0c00437,
[22] Chaitali V. Khedkar, Nageshwar D. Khupse, Balu R. Thombare, Pravin R. Dusane, Gaurav Lole, Rupesh S. Devan, Aparna S. Deshpande, Shankar I. Patil, Chemical Physics Letters (2020), https://doi.org/10.1016/j.cplett.2020.137131
[23] Wanquan Jiang, Yufeng Zhou, Yanli Zhang, Shouhu Xuan, and Xinglong Gong, , Dalton Trans. (2012), https://doi.org/10.1039/C2DT12307J,
[24] Q. Chen, H. Wang, Q. Wang, Y. Pan, J. Plasmonics (2018), https://doi.org/10.1051/e3sconf/201911801002,
[25] Altangerel Amarjargal, Leonard D. Tijing, Ik-Tae Im, Cheol Sang Kim, Chemical Engineering Journal (2013), https://doi.org/10.1016/j.cej.2013.04.054
[26] A. Benvidi, S. Jahanbani, Journal of Electroanalytical Chemistry (2016), https://doi.org/10.1016/j.jelechem.2016.02.038
[27] C. H. Liu, Z. D. Zhou, D. Xiao, Inorganic Materials (2008), https://doi.org/10.1134/S002016850803014X.
[28] M. Ghazanfari, F. Johar, A. Yazdani, Journal of Ultrafine Grained and Nanostructured Materials (2014), https://doi.org/10.7508/jufgnsm.2014.02.006
[29] Owolabi M. Bankole, and Tebello Nyokong, New J. Chem. (2016), https://doi.org/10.1039/C6NJ01511E
[30] Yufeng Shan, Yong Yang, Yanqin Caoab, and Zhengren Huang, RSC Adv. (2015), https://doi.org/10.1039/C5RA17606A
[31] Ke Gai, Huili Qi, Xiulan Zhu and Mingye Wan, E3S Web Conf. (2019), https://doi.org/10.1051/e3sconf/201911801002
[32] L. Pan, J. Tang, and Y. Chen, Sci. China Chem. (2013), https://doi.org/10.1007/s11426-012-4763-y
[33] Altangerel Amarjargal, Leonard D.Tijing, Ik-TaeIm Cheol, Sang Kim, Chemical Engineering Journal (2013), https://doi.org/10.1016/j.cej.2013.04.054.
[34] Mutasim I.Khalil, Arabian Journal of Chemistry (2015), https://doi.org/10.1016/j.arabjc.2015.02.008
[35] Guozhen Wang, Fei Li, Lan Li, Jiayu Zhao, Xinxuan Ruan, Wenping Ding, Jie Cai, Ang Lu, and Ying Pei, ACS Omega (2020), https://doi.org/10.1021/acsomega.0c00437
[36] F Fajaroh and Nazriati, IOP Conf. Ser.: Mater. Sci. Eng (2017), https://doi.org/10.1088/1757-899X/202/1/012064

[37] R. Ianoș, A. Tăculescu, C. Păcurariu, and I. Lazău, Journal of the American Ceramic Society (2012),) https://doi.org/10.1111/j.1551-2916.2012.05159.x
[38] ElhamTahmasebi, YadollahYamini, Analytica Chimica Acta (2012), https://doi.org/10.1016/j.aca.2012.10.040
[39] Vitalii Patsula, Lucie Kosinová, Marija Lovrić, Lejla Ferhatovic Hamzić, Mariia Rabyk, Rafal Konefal, Aleksandra Paruzel, Miroslav Šlouf, Vít Herynek, Srećko Gajović, and Daniel Horák, ACS Applied Materials & Interfaces (2016) https://doi.org/10.1021/acsami.5b12720
[40] Victor Alfredo Reyes Villegas, Jesús Isaías De León Ramírez, Esteban Hernandez Guevara, Sergio Perez Sicairos, Lilia Angelica Hurtado Ayala, Bertha Landeros Sanchez, Journal of Saudi Chemical Society (2020), https://doi.org/10.1016/j.jscs.2019.12.004.
[41] Sakineh Hashemi Zadeh, Majid Rashidi-Huyeh, and Bruno Palpant, Journal of Applied Physics (2017), https://doi.org/10.1063/1.4997276.
[42] E. Prodan, C. Radloff, N. J. Halas, P. Nordlander, Science (2003) https://doi.org/10.1126/science.1089171
[43] E. Prodan and P. Nordlande, J. Chem. Phys. (2004), https://doi.org/10.1063/1.1647518
[44] Nikolai V. Voshchinnikov, John S. Mathis, THE ASTROPHYSICAL JOURNAL, 526, 257-264(1999).
[45]Carly S. Levin, Cristina Hofmann, Tamer A. Ali, Anna T. Kelly, Emilia Morosan, Peter Nordlander, Kenton H. Whitmire, and Naomi J. Halas, ACS Nano (2009) https://doi.org/10.1021/nn900118a.